

# NJC

Accepted Manuscript



This is an *Accepted Manuscript*, which has been through the Royal Society of Chemistry peer review process and has been accepted for publication.

*Accepted Manuscripts* are published online shortly after acceptance, before technical editing, formatting and proof reading. Using this free service, authors can make their results available to the community, in citable form, before we publish the edited article. We will replace this *Accepted Manuscript* with the edited and formatted *Advance Article* as soon as it is available.

You can find more information about *Accepted Manuscripts* in the [Information for Authors](#).

Please note that technical editing may introduce minor changes to the text and/or graphics, which may alter content. The journal's standard [Terms & Conditions](#) and the [Ethical guidelines](#) still apply. In no event shall the Royal Society of Chemistry be held responsible for any errors or omissions in this *Accepted Manuscript* or any consequences arising from the use of any information it contains.

## ARTICLE

## Cluster- and chain-based magnetic MOFs derived from 3d metal ions and 1,3,5-benzenetricarboxylate

Cite this: DOI: 10.1039/x0xx00000x

Sui-Jun Liu,<sup>ab</sup> Song-De Han,<sup>b</sup> Ze Chang<sup>b\*</sup> and Xian-He Bu<sup>b</sup>

Received 00th XXXX 2015,

Accepted 00th XXXX 2015

DOI: 10.1039/x0xx00000x

www.rsc.org/

Assembly of distinct 3d metal ions with a triangular 1,3,5-benzenetricarboxylic acid (H<sub>3</sub>BTC) generates three new metal-organic frameworks, namely {[Co<sub>3</sub>Na(BTC)<sub>2</sub>(μ<sub>3</sub>-OH)(H<sub>2</sub>O)<sub>3</sub>(DMAc)] H<sub>2</sub>O 0.5DMAc}<sub>n</sub> (**1**), {[Ni<sub>3</sub>(BTC)<sub>2</sub>(μ<sub>3</sub>-OH)(H<sub>2</sub>O)<sub>3</sub>] 2H<sub>2</sub>O · DMAc}<sub>n</sub> (**2**) and {[NH<sub>2</sub>(CH<sub>3</sub>)<sub>2</sub>]<sub>2</sub>[Mn<sub>3</sub>(BTC)<sub>2</sub>(CH<sub>3</sub>COO)<sub>2</sub>] · DMAc}<sub>n</sub> (**3**) (DMAc = *N,N'*-dimethylacetamide). Complexes **1** and **2** show Co<sub>3</sub>/Ni<sub>3</sub> cluster based three-dimensional (3D) frameworks with (3,7)-connected new topology and (3,6)-connected *sit* topology, respectively, while complex **3** reveals 3D framework composed of one-dimensional rod-shaped sinusoidal-like Mn<sup>II</sup>-chains. Magnetic investigation shows that **1–3** display antiferromagnetic behaviors although they feature different spin carriers and linkage modes of spin carriers.

## Introduction

Recently, metal-organic frameworks (MOFs) as an intriguing class of crystalline materials have attracted significant attention due to their diverse structures and remarkable performances in numerous areas such as gas storage and separation, magnetism, catalysis, and sensing applications.<sup>1</sup> It has been proved that the structures and properties of MOFs is mainly determined by its intrinsic organic linkers, inorganic metal units as well as the external synthesis conditions.<sup>2</sup> To construct desirable magnetic MOFs, metal clusters and chains are preferred motifs since the magnetic exchange between the metal ions in these fragments could be enhanced through the rational choice of bridging ligands. Thus, cluster- and chain-based MOFs as low-dimensional magnets including single-molecule magnets and single-chain magnets could be realized by choosing short bridging groups such as N<sub>3</sub><sup>-</sup>, RCOO<sup>-</sup> and CN<sup>-</sup> et al.<sup>3</sup> Considerable interest has been focused on the study of these low-dimensional magnets because of their potential applications in information storage and quantum computing at the molecular level.

On the other hand, multicarboxylate ligands are promising candidates for the synthesis of functional MOFs owing to the diversity of the coordination modes of carboxylate groups to metal ions and the various backbones available.<sup>4</sup> As a tricarboxylate ligand, 1,3,5-benzenetricarboxylic acid (H<sub>3</sub>BTC) has been extensively investigated for the construction of functional MOFs.<sup>5</sup> Its rigid triangle backbone and versatile coordination modes of carboxylate could benefit the assembly of three dimensional (3D) MOFs with unique topologies and properties.<sup>6</sup> However, compared with the numerous researches of BTC-based MOFs on their porosity and topology, the

research of magnetic properties are quite limited, especially for the MOFs with polynuclear clusters or chains as building units.<sup>7</sup>

Herein, as an expansion of our studies on the synthesis and properties of cluster- and chain-based MOFs,<sup>8</sup> we describe the synthesis, structures and magnetism of three new MOFs based on H<sub>3</sub>BTC with the formulae {[Co<sub>3</sub>Na(BTC)<sub>2</sub>(μ<sub>3</sub>-OH)(H<sub>2</sub>O)<sub>3</sub>(DMAc)] H<sub>2</sub>O 0.5DMAc}<sub>n</sub> (**1**), {[Ni<sub>3</sub>(BTC)<sub>2</sub>(μ<sub>3</sub>-OH)(H<sub>2</sub>O)<sub>3</sub>] 2H<sub>2</sub>O · DMAc}<sub>n</sub> (**2**), and {[NH<sub>2</sub>(CH<sub>3</sub>)<sub>2</sub>]<sub>2</sub>[Mn<sub>3</sub>(BTC)<sub>2</sub>(CH<sub>3</sub>COO)<sub>2</sub>] · DMAc}<sub>n</sub> (**3**) (DMAc = *N,N'*-dimethylacetamide). All these BTC-supported MOFs possess 3D framework structure. Complexes **1** and **2** feature triangular Co<sub>3</sub>/Ni<sub>3</sub> building units connected by carboxylates and μ<sub>3</sub>-OH bridges, while **3** possesses rod-shaped sinusoidal-like Mn<sup>II</sup>-chains bridged by acetate and carboxylate. Besides the studies on the structures and topologies of these MOFs, attention is paid to the investigation of their magnetism, and magnetic analysis indicates that **1–3** show antiferromagnetic coupling between the metal centers.

## Experimental

## Materials and instrumentation

All chemicals were commercially available and used as received. IR spectra were measured on a TENSOR 27 (Bruker) FT-IR spectrometer with KBr pellets in the range of 4000–400 cm<sup>-1</sup>. Elemental analyses of C, H and N were performed on a Perkin-Elmer 240C analyzer. The PXRD spectra were recorded on a Bruker D8 Focus diffractometer for a Cu-target tube and a graphite monochromator. Simulation of the PXRD spectra were carried out by the single-crystal data and diffraction-crystal module of the Mercury (Hg) program available free of charge. Magnetic data were collected using crushed crystals of the

sample on a Quantum Design MPMS-XL-7 SQUID magnetometer equipped. The data were corrected using Pascal's constants to calculate the diamagnetic susceptibility, and an experimental correction for the sample holder was applied.

#### Synthesis of complexes

**{[Co<sub>3</sub>Na(BTC)<sub>2</sub>(μ<sub>3</sub>-OH)(H<sub>2</sub>O)<sub>3</sub>(DMAc)] H<sub>2</sub>O 0.5DMAc}<sub>n</sub> (1).** A mixture of Co(NO<sub>3</sub>)<sub>2</sub> 6H<sub>2</sub>O (29.1 mg, 0.1 mmol), NaCl (116 mg, 2 mmol), and H<sub>3</sub>BTC (105 mg, 0.5 mmol) in 10 mL component solvent (DMAc : H<sub>2</sub>O = 4 : 1) was sealed in a 23 mL Teflon-lined autoclave and heated to 100 °C for 2 days. After the autoclave was cooled to room temperature in 24 h, purple block crystals suitable for single crystal X-ray crystallographic analysis were obtained. Yield: ~40% based on H<sub>3</sub>BTC. Anal. Calcd for C<sub>56</sub>H<sub>75</sub>Co<sub>6</sub>N<sub>5</sub>Na<sub>2</sub>O<sub>39</sub>: C, 36.51; H, 4.10; N, 3.80%. Found: C, 36.87; H, 4.55; N, 2.83%. IR (KBr, cm<sup>-1</sup>): 3123w, 2918w, 2166m, 1589s, 1538s, 1400s, 1218w, 1058m, 1013s, 859s, 814s, 791s, 768s, 705m, 626m.

**{[Ni<sub>3</sub>(BTC)<sub>2</sub>(μ<sub>3</sub>-OH)(H<sub>2</sub>O)<sub>3</sub>] 2H<sub>2</sub>O DMAc}<sub>n</sub> (2).** A mixture of Ni(NO<sub>3</sub>)<sub>2</sub> 6H<sub>2</sub>O (291 mg, 1 mmol), NaCl (116 mg, 2 mmol), and H<sub>3</sub>BTC (105 mg, 0.5 mmol) in 10 mL component solvent

(DMAc : H<sub>2</sub>O = 4 : 1) was sealed in a Teflon-lined autoclave and heated to 90 °C for 2 days. After the autoclave was cooled to room temperature in 12 h, green block crystals suitable for single crystal X-ray crystallographic analysis were obtained. Yield: ~10% based on H<sub>3</sub>BTC. Anal. Calcd for C<sub>22</sub>H<sub>26</sub>Ni<sub>3</sub>NO<sub>19</sub>: C, 33.68; H, 3.34; N, 1.79%. Found: C, 33.23; H, 3.75; N, 1.34%. IR (KBr, cm<sup>-1</sup>): 3432s, 2950w, 1686s, 1631s, 1533m, 1436m, 1382s, 1220w, 1108w, 768w, 715w.

**{[NH<sub>2</sub>(CH<sub>3</sub>)<sub>2</sub>]<sub>2</sub>[Mn<sub>3</sub>(BTC)<sub>2</sub>(CH<sub>3</sub>COO)<sub>2</sub>] DMAc}<sub>n</sub> (3).** A mixture of Mn(HCOO)<sub>2</sub> 4H<sub>2</sub>O (217 mg, 1 mmol) and H<sub>3</sub>BTC (105 mg, 0.5 mmol) in 10 mL component solvent (DMAc : H<sub>2</sub>O = 4 : 1) was sealed in a Teflon-lined autoclave and heated to 150 °C for 3 days. After the autoclave was cooled to room temperature in 12 h, pink block crystals suitable for single crystal X-ray crystallographic analysis were obtained. Yield: ~45% based on H<sub>3</sub>BTC. Anal. Calcd for C<sub>30</sub>H<sub>37</sub>Mn<sub>3</sub>N<sub>3</sub>O<sub>17</sub>: C, 41.11; H, 4.26; N, 4.79%. Found: C, 41.56; H, 4.63; N, 4.35%. IR (KBr, cm<sup>-1</sup>): 3432s, 2948w, 2166m, 1690s, 1633s, 1532m, 1433m, 1384s, 1220w, 1108w, 773w, 717w.

**Table 1.** Crystal data and structure refinement parameters for complexes 1–3.

	1	2	3
Formula	C <sub>56</sub> H <sub>75</sub> Co <sub>6</sub> N <sub>5</sub> Na <sub>2</sub> O <sub>39</sub>	C <sub>22</sub> H <sub>26</sub> Ni <sub>3</sub> NO <sub>19</sub>	C <sub>30</sub> H <sub>37</sub> Mn <sub>3</sub> N <sub>3</sub> O <sub>17</sub>
<i>Mr</i> (g mol <sup>-1</sup> )	1841.77	784.52	876.44
crystal system	Monoclinic	Orthorhombic	Orthorhombic
space group	<i>C</i> 2	<i>Imm</i> 2	<i>Pbcm</i>
a [Å]	18.125(4)	9.787(2)	12.692(3)
b [Å]	12.106(2)	12.157(2)	14.424(3)
c [Å]	17.733(4)	15.182(3)	21.492(4)
β [°]	107.30(3)	90	90
V [Å <sup>3</sup> ]	3715.1(13)	1806.5(6)	3934.5(14)
Z	2	2	4
D <sub>calcd</sub> [g cm <sup>-3</sup> ]	1.646	1.214	1.177
μ [mm <sup>-1</sup> ]	1.418	1.599	1.000
F (000)	1884	666	1388
Reflns collected/unique	19250/8441	9545/2286	31002/3564
data/restraints/parameters	8441/111/525	2286/1/97	3564/0/194
GOF on F <sup>2</sup>	1.073	1.118	1.151
R <sub>1</sub> <sup>a</sup> /wR <sub>2</sub> <sup>b</sup> [I>2σ(I)]	0.0691/0.1757	0.0323/0.0769	0.0845/0.1843
R <sub>int</sub>	0.1164	0.0446	0.153

$${}^a R_1 = \sum ||F_o| - |F_c|| / \sum |F_o|; {}^b wR_2 = \{ \sum [w(F_o^2 - F_c^2)^2] / \sum w(F_o^2)^2 \}^{1/2}.$$

#### Crystallographic data collection and refinement

All diffraction data were collected on a Rigaku SCX-mini diffractometer at 293(2) K with Mo-K $\alpha$  radiation ( $\lambda = 0.71073$  Å) by  $\omega$  scan mode. The program *CrystalClear*<sup>11</sup> was used for integration of the diffraction profiles. The structures were solved by direct methods using the SHELXS program of the SHELXTL package and refined by full-matrix least-squares methods with SHELXL (semi-empirical absorption corrections were applied using SADABS program).<sup>12</sup> The positions of metal atoms were located from *E*-map by direct-method, and other non-hydrogen atoms were located in difference Fourier syntheses and least-squares refinement cycles, and finally refined anisotropically. The hydrogen atoms of the ligands were placed theoretically onto the specific atoms and refined isotropically as riding atoms. The hydrogen atoms of the coordinated water for **1** and **2** and the hydrogen atoms of the bridging hydroxyl anions for **1** were included in the molecular formula directly. The restraint instruments (isor, delu, dfix, flat) were used in the refinement of **1** to make the parameters of coordinated DMAc reasonable. The disordered solvent molecules and dimethylamine cations in **2** and **3** are removed by SQUEEZE as implemented in PLATON.<sup>13</sup> Details of the crystal data collection and refinement parameters for **1–3** are given in Table 1. Selected bond lengths and angles are given in Tables S3–S5 (ESI). Full crystallographic data for **1–3** have been deposited with the CCDC numbers 917757–917759, which are available from The Cambridge Crystallographic Data Centre via [www.ccdc.cam.ac.uk/data\\_request/cif](http://www.ccdc.cam.ac.uk/data_request/cif).

## Results and discussion

### Synthesis and characterization

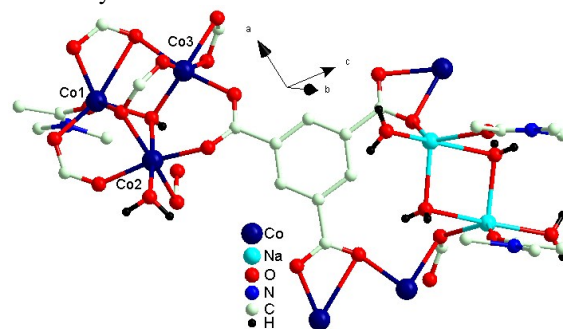
Generally, BTC<sup>3-</sup> ligand with three carboxylate groups is an excellent candidate in synthesizing cluster- and chain-based MOFs. In our efforts to obtain complexes **1–3**, the metal salts, solvents, and reaction temperature have been altered. Notably, acetate anions and dimethylamine cations in **3** are *in situ* generated due to the decomposition of DMAc molecules. Besides the choice of ligands, reacting conditions, especially solvents and temperature, could also affect the structures of target complexes.<sup>9</sup> To investigate the influence of solvents and temperature for solvothermal reaction, other conditions such as counter anions, the pH values of the reaction solutions and molar ratio between reactants should remain unchanged. Thus the investigation on the relationship between reacting conditions and the final structures can help us better understand which reaction conditions facilitate the formation of desired structures. In this paper, temperature ranges from 90 °C to 160 °C and common solvents were used. Notably, high temperature is favorable for the *in situ* decomposition of DMAc molecules to generate dimethylamine cation.<sup>10</sup>

Different methods has been tried to synthesize **1** and **2**, i.e., CoCl<sub>2</sub> and NiCl<sub>2</sub> as the metal ions source, and the precipitate were obtained. According to the reported literatures,<sup>14</sup> NaCl has been successfully used to construct clusters and cluster-based MOFs. In order to further investigate the role of NaCl in the synthesis of MOF **1** and **2**, three similar reactions have been carried out, including the addition of none assistant reagent,

NaNO<sub>3</sub> and KCl. The results show that Na<sup>+</sup> as a template takes a key role in the construction of **1** and **2**, however, Na<sup>+</sup> has taken part in coordination in **1** not in **2**. In addition, the addition of NaCl has a negative effect on the synthesis of MOF **3** (see Table S2, ESI).

Complexes **1–3** are 3D structures supported by BTC<sup>3-</sup> with Co<sub>3</sub> and Na<sub>2</sub> clusters, Ni<sub>3</sub> clusters, and 1D rod-shaped sinusoidal-like Mn-chains as building units, respectively. The detailed structural information was discussed as below.

Complex **1** crystallizes in the monoclinic space group *C*2. The asymmetric unit of **1** consists of three occupied Co<sup>II</sup> ion, one Na<sup>I</sup> ion, two fully deprotonated BTC<sup>3-</sup>, one  $\mu_3$ -OH<sup>-</sup>, three coordinated H<sub>2</sub>O, one coordinated DMAc, one lattice H<sub>2</sub>O molecule and half of an occupied lattice DMAc. The hexa-coordinated cobalt ions are in irregular octahedron geometry (Fig. 1). The Co1 center is surrounded by six O atoms from one DMAc molecules, one  $\mu_3$ -OH<sup>-</sup> and three carboxylates. The Co2 ion is coordinated by four O atoms from BTC<sup>3-</sup> ligands, one O atom from  $\mu_3$ -OH<sup>-</sup> and one water O atom, while the hexa-coordinated Co3 ion is finished by the coordination of one O atom of  $\mu_3$ -OH<sup>-</sup> and five carboxylate O atoms. The Co-O bond lengths are in the range of 1.978(6)–2.221(7) Å (Table S2, ESI). The neighboring Co<sup>II</sup> centers are bridged by  $\mu_3$ -OH<sup>-</sup> and carboxylate groups with *syn-syn*- $\mu_2$ - $\eta^1$ : $\eta^1$ , *syn-syn*- $\mu_2$ - $\eta^1$ : $\eta^2$  and *syn-syn-syn*- $\mu_3$ - $\eta^1$ : $\eta^2$  bridging modes to form triangular trimeric Co<sup>II</sup> units [Co<sub>3</sub>( $\mu_3$ -OH)(CO<sub>2</sub>)<sub>6</sub>(H<sub>2</sub>O)(DMAc)] (Fig. 1). In addition, the NaI ion exhibits five-coordinate environment with three water O atoms, one DMAc and one carboxylate O atom. Therefore, the adjacent Na<sup>I</sup> ions are bridged by two water molecules to form a Na<sub>2</sub> metal centre. Each carboxylate of BTC<sup>3-</sup> ligands coordinates with three Co<sub>3</sub> clusters and one Na<sub>2</sub> metal centre to extend the clusters into 3D framework (Fig. 1). Topologically, the Co<sub>3</sub> clusters and BTC<sup>3-</sup> ligands could be simplified as 7-connected and 3-connected nodes, respectively, and the whole framework show a (3,7)-connected new topology network with a point symbol of {3.5.6}{3<sup>2</sup>.4<sup>2</sup>.5<sup>3</sup>.6<sup>10</sup>.7<sup>3</sup>.8}{4.5.6} rationalized by TOPOS 4.0<sup>15</sup>.



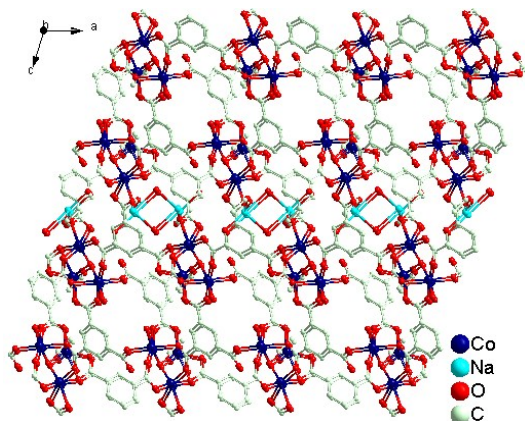


**Fig. 1** Views of the coordination environment of  $\text{Co}^{\text{II}}$  ions in **1** (top); the 3D structure of **1** (bottom). H atoms are omitted for clarity (similarly hereafter).

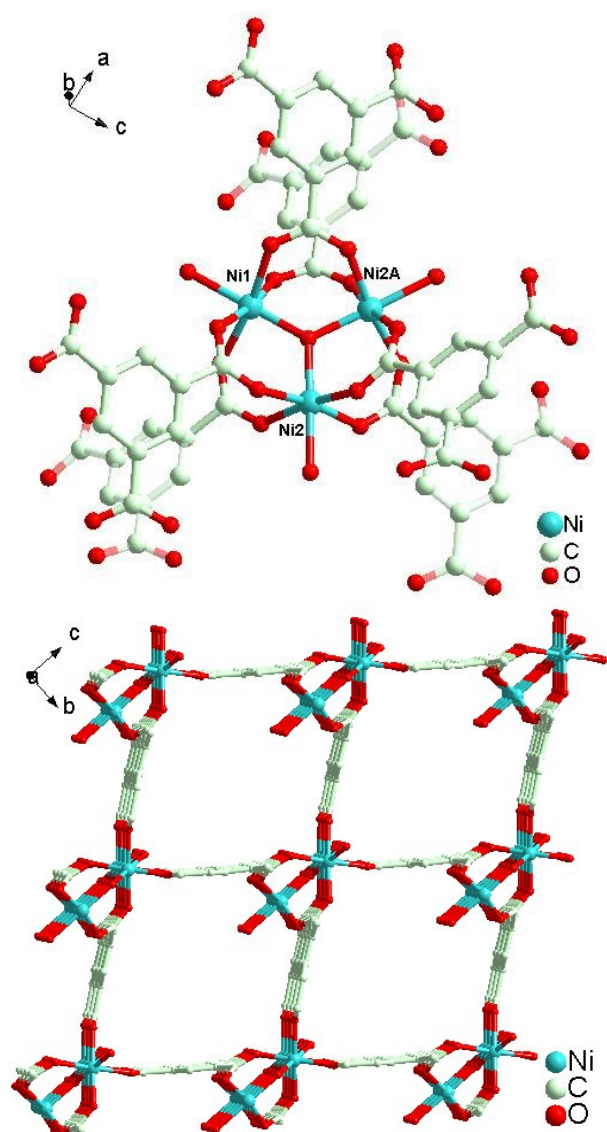


**Fig. 2** Views of the coordination environment of nickel ions in **2** (top); the 3D structure of **2** (bottom).

Crystallographic studies reveal that complex **2** crystallizes in an orthorhombic system with space group  $Imm2$ . The asymmetric unit consists of one occupied  $\text{Ni}^{\text{II}}$  ions, a half occupied  $\text{Ni}^{\text{III}}$  ions, one  $\text{BTC}^{3-}$  ligand, a half  $\mu_3\text{-OH}^-$  and one and a half coordinated  $\text{H}_2\text{O}$ . All  $\text{Ni}^{\text{II}}$  ions are located in six coordinated environments with six O atoms from one water molecule, one  $\mu_3\text{-OH}^-$  and four carboxylate of  $\text{BTC}^{3-}$  ligands (the range of Ni-O length: 1.935(5)-2.116(4) Å, see Table S3, ESI). The adjacent nickel centers are bridged by  $\mu_3\text{-OH}^-$  and carboxylate groups with  $\text{syn-syn-}\mu_2\text{-}\eta^1\text{:}\eta^1$  bridging mode to form mixed-valence triangular  $\text{Ni}_3$  units  $[\text{Ni}_2^{\text{II}}\text{Ni}^{\text{III}}(\mu_3\text{-OH})(\text{CO}_2)_6(\text{H}_2\text{O})_3]$  (Fig. 2). The valence of the nickel ions was further confirmed by the bond valence sum (Table S1, ESI) and the magnetic data (vide infra). Similar to the connection mode in **1**, each carboxylate of the  $\text{BTC}^{3-}$  ligand in **2** links one  $\text{Ni}_3$  cluster, and each  $\text{Ni}_3$  unit connects twelve neighboring units through six  $\text{BTC}^{3-}$  ligands to give rise to the final 3D framework (Fig. 2). Therefore, the framework of **2** could also be rationalized to a (3,6)-connected *sit* topology network with  $\text{Ni}_3$  clusters and  $\text{BTC}^{3-}$  ligands as 6-connected and 3-connected nodes, respectively.

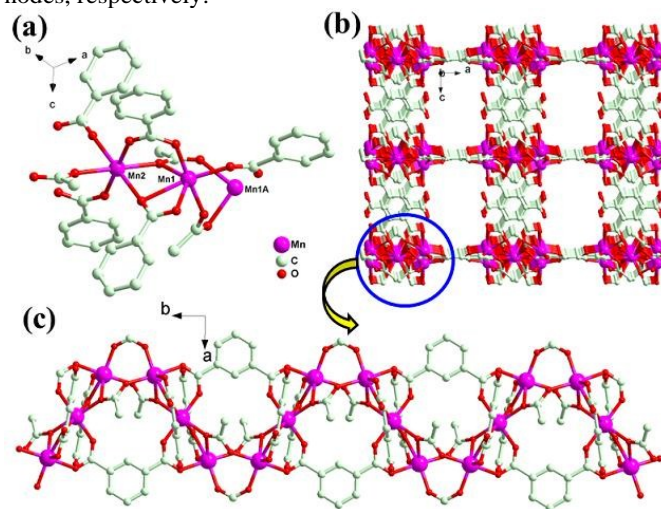


**Fig. 3** Views of (a) the coordination environment of  $\text{Mn}^{\text{II}}$  ions in **3**; (b) the 3D structure of **3**; (c) the 1D chain in **3**.

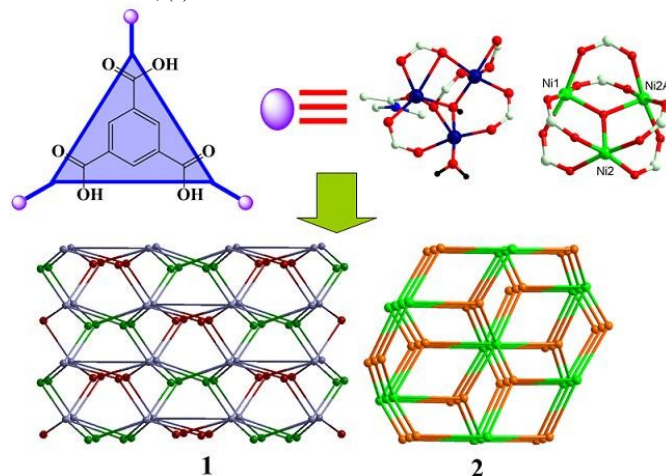


**Fig. 4** The topological analysis and representations of **1** and **2**.

Complex **3** crystallizes in the space group *Pbcm* of orthorhombic system, and the crystallographic asymmetric unit consists of one occupied Mn1, a half occupied Mn2, one BTC<sup>3-</sup> ligands and one OAc<sup>-</sup> anion (Fig. 3a). The Mn1 center exhibits a hexa-coordinated environment with two O atoms from two acetate anions and four O atoms from three different BTC<sup>3-</sup> ligands. The Mn2 ion adopts distorted octahedron geometry with two O atoms of two acetate anions and four O atoms of four different BTC<sup>3-</sup> ligands. Mn1 and Mn2 are bridged by acetate anions and carboxylate groups of BTC<sup>3-</sup> ligands to form 1D rod-shaped sinusoidal-like Mn-chains (Fig. 3c), which is further linked to neighboring 1D chains to result in a 3D anionic framework structure (Fig. 3b). The charge is balanced by the *in situ* generated dimethylamine cation from the decomposition of solvent DMAc.

Generally, the  $\mu_3$ -OH<sup>-</sup> group is helpful for the formation of the metal cluster-based units. In addition, the BTC<sup>3-</sup> ligands and metal cluster-based units could serve as 3-connected and high-connected nodes, respectively. Therefore, (3,*n*)-connected topology network could be anticipated (Fig. 4).

For complexes **1-3**, PXRD has been used to check the phase purities of the magnetic samples in the solid state, as shown in Fig. S1 (ESI). The measured PXRD patterns closely match with the simulated patterns generated from the results of single-crystal diffraction data respectively, indicates the identical structure of the bulk sample and the single crystal tested. It is noteworthy that the preferred orientation of the lattice face and the crystallinity of target MOFs may be mainly responsible for the peak intensity differences between the experimental values and the simulated ones.<sup>17</sup>

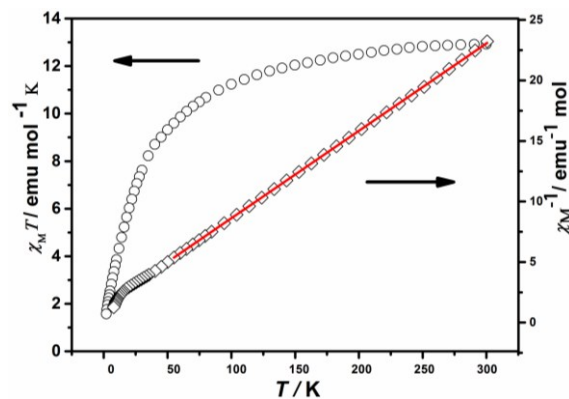
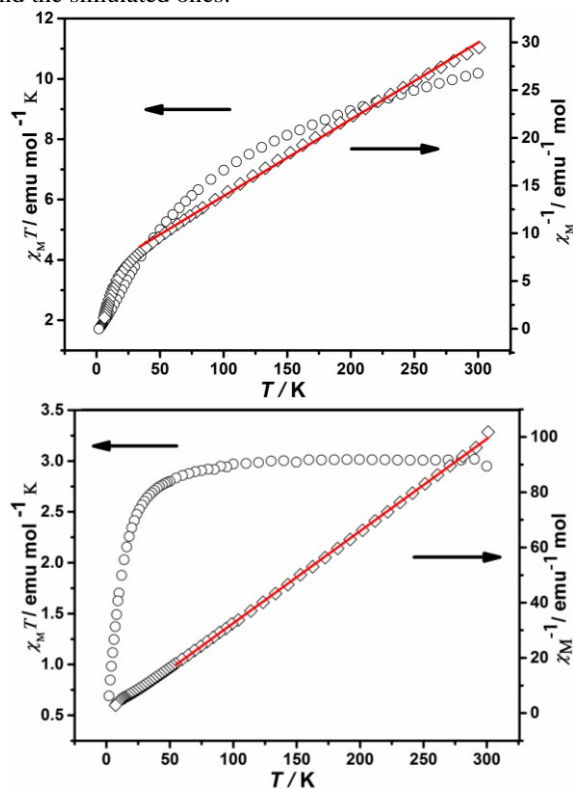


Fig. 5 The  $\chi_M T$  vs.  $T$  and  $\chi_M^{-1}$  vs  $T$  (red part for the Curie-Weiss fitting) plots for **1** (top), **2** (middle) and **3** (bottom).

### Magnetic properties

The magnetic properties of **1-3** were investigated by solid state magnetic susceptibility measurements in the 2–300 K range at a field of 1 kOe and the isothermal field-dependent magnetizations  $M(H)$  at 2 K (All the measurements were carried out on crushed crystalline samples). Complexes **1-3** display overall antimagnetic (AF) behaviours as below.

For **1** and **2**, the magnetic properties in the form of  $\chi_M T$  vs.  $T$  plots are shown in Fig. 5. At room temperature, the  $\chi_M T$  value of **1** is 10.18 emu mol<sup>-1</sup> K, which is much larger than expected spin-only value (5.63 emu mol<sup>-1</sup> K) for three magnetically isolated Co<sup>II</sup> ions ( $S = 3/2$ ,  $g = 2$ ) because of the strong spin-orbit coupling of octahedral Co<sup>II</sup> ion, while the  $\chi_M T$  value of **2** is 2.95 emu mol<sup>-1</sup> K, which is slightly larger than expected spin-only value 2.38 emu mol<sup>-1</sup> K for three magnetically isolated nickel ions (two Ni<sup>II</sup> ions with  $S = 1$ ,  $g = 2$  and one Ni<sup>III</sup> ions with  $S = 1/2$ ,  $g = 2$ ) due to the orbital contributions of the octahedral nickel ions. For **1** and **2**, as the temperature decreases, the value of  $\chi_M T$  slowly decreases down to minimum values of 1.71 and 0.69 emu mol<sup>-1</sup> K at 2 K, respectively, indicating AF coupling between metal centers, which is further confirmed by the negative Weiss constant  $\theta = -78.08$  K for **1** and  $\theta = -2.87$  K for **2** derived from Curie-Weiss fitting [ $\chi_M = C/(T-\theta)$ ] of the magnetic data over the temperature range 30–300 K for **1** and 50–300 K for **2**. The negative  $\theta$  for **1** is less than  $-20$  K, suggesting AF interactions mediated by BTC and  $\mu_3$ -OH<sup>-</sup> between Co<sup>II</sup> ions.<sup>16</sup> The  $M$  vs.  $H$  plots (at 2 K) for **1** and **2** are shown in Fig. S2 (ESI) and also support the conclusion.  $M$  increases slowly and reaches 2.75 N $\beta$  and 2.56 N $\beta$  at 70 kOe, respectively, far from the saturation values. In **1** and **2**, since the intertrimer M $\cdots$ M ( $M = \text{Co, Ni}$ ) distances linked by BTC<sup>3-</sup> ligands are considerably longer than the intratrimer M $\cdots$ M separation, the intertrimer exchange interactions can be seen approximately as the effect of the molecular field. Therefore, the BTC ligands only transmitted neglectable intercluster AF interactions.<sup>18</sup>

The magnetic properties of **3** calculated as  $\chi_M T$  vs  $T$  and  $\chi_M^{-1}$  vs  $T$  plots are shown in Fig. 5. The  $\chi_M T$  value of **3** at 300 K is 12.92 emu mol<sup>-1</sup> K, which agrees with the values of three isolated Mn<sup>II</sup> ions (13.13 emu mol<sup>-1</sup> K). The  $\chi_M T$  decreases

gradually on cooling and reaches a minimum value of 1.58 emu mol<sup>-1</sup> K at 2 K, indicative of AF couplings between Mn<sup>II</sup> centers, which is further corroborated by the negative  $\theta = -25.55$  K from the Curie-Weiss fit of the magnetic data between 50-300 K. The AF couplings between Mn<sup>II</sup> ions is also supported by the field-dependent magnetization at 2 K (Fig. S2c, ESI), in which the reduced magnetization displays a quasi-linear increasing trend along with the external fields and final reaches 4.09 N $\beta$  at 45 kOe, far from the saturation value. As mentioned above, complexes **1–3** exhibit AF behaviors although their connection modes between metal ions are not the same.

As is known, the *syn-syn*- $\mu_2$ - $\eta^1$ : $\eta^1$  (probably producing antiferromagnetism between 3d metal ions), *syn-anti*- $\mu_2$ - $\eta^1$ : $\eta^1$  (likely producing weak ferromagnetism) and  $\mu_2$ - $\eta^2$  types are usual coordination modes of carboxylate groups to transfer magnetism. In this work, all the carboxylate groups of BTC<sup>3-</sup> ligands and OAc<sup>-</sup> anions exhibit *syn-syn* mode, which play the dominant role of antiferromagnetic interactions between metal centres.

To our best knowledge, similar cluster- and chain-based 3d metal complexes with H<sub>3</sub>BTC are very limited, and their magnetism has been less studied. Kou and coworkers have reported a 2D complex [Ni<sub>3</sub>(BTC)<sub>2</sub>( $\mu$ -H<sub>2</sub>O)<sub>2</sub> 6H<sub>2</sub>O],<sup>7c</sup> which possesses an infinite double-layered structure. The layer is composed of *syn-syn* carboxylate- and aqua oxygen-bridged Ni<sub>3</sub> units that are further connected by BTC<sup>3-</sup>. Magnetic investigation that ferromagnetic coupling is operative between the Ni<sup>II</sup> ions through the *syn-syn* carboxylate bridges because the magnetic exchange through the aqua bridges [Ni-O-Ni bond angle = 122.8(3)°] is antiferromagnetic. Another example is that Stride and coworkers have reported two pairs of isostructural chain-based MOFs derived from BTC<sup>3-</sup> ligands.<sup>7b</sup> Two of these compounds (**a** and **b**) are characterized by unique fluoride bridged 1D chains, whilst the other two compounds (**c** and **d**) are constructed *via* a complex hydrogen bonding network. Magnetic data indicates that there are strong antiferromagnetic couplings among metal atoms within the 1D fluoride chains in both **a** and **b**, whilst only moderate antiferromagnetic interactions among Co<sup>II</sup> ions in **d**. Compared with these complexes, MOFs in this work includes  $\mu_3$ -OH groups or acetates, leading to antiferromagnetic couplings between metal centres.

## Conclusions

By employing 1,3,5-benzenetricarboxylate as 3-connected ligand, three metal-organic frameworks based on 3d metal ions have been successfully obtained under solvothermal conditions. Structural analysis indicates that they are all three-dimensional structure. Complexes **1** and **2** display (3,7)-connected new topology and (3,6)-connected *sit* topology, respectively, with triangular M<sub>3</sub> (M = Co, Ni) cluster as building units, while one-dimensional rod-shaped sinusoidal-like Mn<sup>II</sup>-chains serve as building units in **3**. Magnetic measurements imply that **1–3** exhibit antiferromagnetic behaviors although their spin carriers

and linkage modes of spin carriers are different. This work not only enriches the existing field of BTC-supported metal-organic frameworks, but also provides a case of systematic investigation of magnetic properties of metal-organic frameworks. Further studies will concentrate on the investigation of their other properties to create multifunctional materials, as well as an extension of these synthetic methods into other related systems to prepare magnetic metal-organic frameworks.

## Acknowledgements

This work was supported by 973 Program of China (2014CB845600), the National Science Foundation of China (21501077, 21290171, 21421001 and 21202088), MOE Innovation Team of China (IRT13022), the Postdoctoral Preferred Project Fund of Jiangxi Province (2015KY34), and the Natural Science Foundation of Jiangxi Province of China (20151BAB213003). We also thank Dr. Feng-Feng Wang at Beijing National Laboratory for Molecular Sciences for crystal structure refinements.

## Notes and references

<sup>a</sup>School of Metallurgy and Chemical Engineering, and Engineering Research Center of High-Efficiency Development and Application Technology of Tungsten Resource, Jiangxi University of Science and Technology, Ganzhou 341000, Jiangxi Province, P.R. China.

<sup>b</sup>School of Materials Science and Engineering, TKL of Metal- and Molecule-Based Material Chemistry and Collaborative Innovation Center of Chemical Science and Engineering (Tianjin), Nankai University, Tianjin 300071, P.R. China.

E-mail: changze@nankai.edu.cn. Fax: +86-22-23502458.

Electronic Supplementary Information (ESI) available: Crystallographic data files (CIF), simulated and experimental PXRD (Fig. S1) of **1–3**, magnetic data (Fig. S2) of **1–3**, bond valence sum (Table S1) and selected bond distances and angles for **1–3** (Tables S2–S4).

- (a) J. R. Li, J. Sculley and H. C. Zhou, *Chem. Rev.*, 2012, **112**, 869; (b) J. Zhang, L. Wojtas, R. W. Larsen, M. Eddaoudi and M. J. Zaworotko, *J. Am. Chem. Soc.*, 2009, **131**, 17040; (c) Y. B. Zhang, W. X. Zhang, F. Y. Feng, J. P. Zhang and X. M. Chen, *Angew. Chem., Int. Ed.*, 2009, **48**, 5287; (d) Q. Chen, Z. Chang, W. C. Song, H. Song, H. B. Song, T. L. Hu and X. H. Bu, *Angew. Chem. Int. Ed.*, 2013, **52**, 11550; (e) J. Lu, D. R. Turner, L. P. Harding, L. T. Byrne, M. V. Baker and S. R. Batten, *J. Am. Chem. Soc.*, 2009, **131**, 10372; (f) F. S. Guo, Y. C. Chen, J. L. Liu, J. D. Leng, Z. S. Meng, P. Vrabel, M. Orendáč and M. L. Tong, *Chem. Commun.*, 2012, **48**, 12219; (g) W. Liu, X. Bao, L. L. Mao, J. Tucek, R. Zboril, J.-L. Liu, F. S. Guo, Z. P. Ni and M. L. Tong, *Chem. Commun.*, 2014, **50**, 4059; (h) E. Coronado and G. M. Espallargas, *Chem. Soc. Rev.* 2013, **42**, 1525; (i) R. Ricco, L. Malfatti, M. Takahashi, A. J. Hill and P. Falcaro, *J. Mater. Chem. A*, 2013, **1**, 13033.
- For examples, see (a) M. E. Robinson, J. E. Mizzi, R. J. Staples and R. L. LaDuca, *Cryst. Growth Des.*, 2015, **15**, 2260; (b) X. Rao, T. Song, J. Gao, Y. Cui, Y. Yang, C. Wu, B. Chen and G. Qian, *J. Am. Chem. Soc.*, 2013, **135**, 15559; (c) J. W. Uebler, A. L. Pochodylo, R. J. Staples and R. L. LaDuca, *Cryst. Growth Des.*, 2013, **13**, 2220; (d) Q.

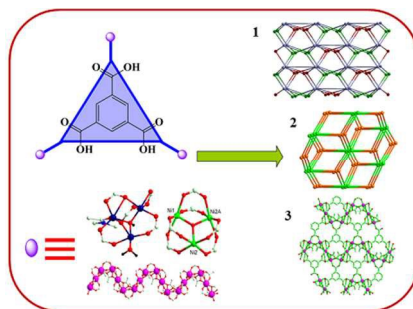
- Zhao, X. M. Liu, W. C. Song and X. H. Bu, *Dalton Trans.*, 2012, **41**, 6813; (e) Y. Q. Chen, G. R. Li, Z. Chang, Y. K. Qu, Y. H. Zhang and X. H. Bu, *Chem. Sci.*, 2013, **4**, 3678; (f) M. X. Wang, L. S. Long, R. B. Huang and L. S. Zheng, *Chem. Commun.*, 2011, **47**, 9834; (g) B. Liu, W.-P. Wu, L. Hou and Y. Y. Wang, *Chem. Commun.*, 2014, **50**, 8731; (h) S. Hu, J.-L. Liu, Z.-S. Meng, Y.-Z. Zheng, Y. Lan, A. K. Powell and M.-L. Tong, *Dalton Trans.*, 2011, **40**, 27; (i) Z. Lin and M.-L. Tong, *Coord. Chem. Rev.*, 2011, **255**, 421.
- 3 (a) J. Ribas, A. Escuer, M. Monfort, R. Vicente, R. Cortés, L. Lezama and T. Rojo, *Coord. Chem. Rev.*, 1999, **193-195**, 1027; (b) A. Escuer and G. Aromi, *Eur. J. Inorg. Chem.*, 2006, 4721; (c) Q. Yang, J. P. Zhao, B. W. Hu, X. F. Zhang and X. H. Bu, *Inorg. Chem.*, 2010, **49**, 3746; (d) X. Y. Wang, Z. M. Wang and S. Gao, *Chem. Commun.*, 2007, 1127; (e) Z. G. Gu, Y. F. Xu, X. J. Yin, X. H. Zhou, J. L. Zuo and X. Z. You, *Dalton Trans.*, 2008, 5593; (f) S. D. Han, J. P. Zhao, S. J. Liu and X. H. Bu, *Coord. Chem. Rev.*, 2015, **289-290**, 32.
- 4 (a) M. A. Nadeem, D. J. Craig and J. A. Stride, *Dalton Trans.*, 2010, **39**, 4358; (b) L. Sun, H. Xing, J. Xu, Z. Liang, J. Yu and R. Xu, *Dalton Trans.*, 2013, **42**, 5508.
- 5 (a) V. Stavila, J. Volponi, A. M. Katzenmeyer, M. C. Dixon and M. D. Allendorf, *Chem. Sci.*, 2012, **3**, 1531; (b) O. Kozachuk, K. Yusenko, H. Noei, Y. Wang, S. Walleck, T. Glaser and R. A. Fischer, *Chem. Commun.*, 2011, **47**, 8509; (c) C. Livage, N. Guillou, J. Marrot and G. Férey, *Chem. Mater.*, 2001, **13**, 4387; (d) D. Cheng, M. A. Khan and R. P. Houser, *Cryst. Growth Des.*, 2004, **4**, 599; (e) A. Banerjee, P. Mahata and S. Natarajan, *Eur. J. Inorg. Chem.*, 2008, 3501.
- 6 (a) S. O. H. Gutschke, M. Molinier, A. K. Powell, R. E. P. Winpenny and P. T. Wood, *Chem. Commun.*, **1996**, 823; (b) J. H. He, Y. T. Zhang, Q. H. Pan, J. H. Yu, H. Ding and R. R. Xu, *Microporous Mesoporous Mater.*, 2006, **90**, 145; (c) J. Chen, M. Ohba and S. Kitagawa, *Chem. Lett.*, 2006, 35, 526.
- 7 (a) Y. L. Wang, N. Zhang, Q. Y. Liu, X. Yang, H. Bai, L. Y. Duan and H. Y. Liu, *Inorg. Chem. Commun.*, 2011, **14**, 380; (b) M. A. Nadeem, M. Bhadbhade and J. A. Stride, *Dalton Trans.*, 2010, **39**, 9860; (c) H. J. Yang, A. L. Cui, R. J. Wang and H. Z. Kou, *Chin. J. Chem.*, 2008, **26**, 1527.
- 8 (a) Y. W. Li, J. P. Zhao, L. F. Wang and X. H. Bu, *CrystEngComm*, 2011, **13**, 6002; (b) Y. W. Li, J. R. Li, L. F. Wang, B. Y. Zhou, Q. Chen and X. H. Bu, *J. Mater. Chem. A*, 2013, **1**, 495.
- 9 (a) H. Wang, S. J. Liu, D. Tian, J. M. Jia and T. L. Hu, *Cryst. Growth Des.*, 2012, **12**, 3263; (b) S. D. Han, Y. Q. Chen, J. P. Zhao, S. J. Liu, X. H. Miao, T. L. Hu and X. H. Bu, *CrystEngComm*, 2014, **16**, 753.
- 10 For examples, see (a) F. Yang, Q. Zheng, Z. Chen, Y. Ling, X. Liu, L. Weng and Y. Zhou, *CrystEngComm*, 2013, **15**, 7031; (b) J. P. Zhao, B. W. Hu, F. Lloret, J. Tao, Q. Yang, X. F. Zhang and X. H. Bu, *Inorg. Chem.*, 2010, **49**, 10390; (c) J. D. Lin, X. F. Long, P. Lin and S. W. Du, *Cryst. Growth Des.*, 2010, **10**, 146.
- 11 Rigaku, *Process-Auto*, Rigaku Americas Corporation, The Woodlands, Texas, 1998
- 12 G. M. Sheldrick, *SHELXS97 Program for Solution of Crystal Structures*, University of Göttingen, Göttingen, Germany, 1997.
- 13 A. L. Spek, *J. Appl. Crystallogr.*, 2003, **36**, 7.
- 14 For example, see J.-B. Peng, Q.-C. Zhang, X.-J. Kong, Y.-P. Ren, L.-S. Long, R.-B. Huang, L.-S. Zheng and Z. Zheng, *Angew. Chem., Int. Ed.*, 2011, **50**, 10649-10652.
- 15 V. A. Blatov, *TOPOS, A multipurpose Crystallochemical Analysis with the Program Package*, Samara State University, Russia, 2004.
- 16 (a) M. Kurmoo, *Chem. Soc. Rev.*, 2009, **38**, 1353; (b) J.-P. Zhao, S.-D. Han, R. Zhao, Q. Yang, Z. Chang and X.-H. Bu, *Inorg. Chem.*, 2013, **52**, 2862.
- 17 (a) A. Jeziorna, K. Stopczyk, E. Skorupska, K. Lubierda-Durnas, M. Oszajca, W. Lasocha, M. Górecki, J. Frelek and M. J. Potrzebowski, *Cryst. Growth Des.*, 2015, **15**, 5138; (b) T. Hu, B. Zheng, X. Wang and X. Hao, *CrystEngComm*, 2015, **17**, 9348; (c) S. D. Han, Q. L. Wang, J. Xu, X. H. Bu, *Eur. J. Inorg. Chem.*, 2015, 5379.
- 18 B. W. Sun, S. Gao, B. Q. Ma, D. Z. Niu and Z. M. Wang, *J. Chem. Soc., Dalton Trans.*, 2000, 4187.

## Graphic Abstract

## Graphic Abstract

**Cluster- and chain-based magnetic MOFs derived from 3d metal ions and 1,3,5-benzenetricarboxylate**

Sui-Jun Liu, Song-De Han, Ze Chang\* and Xian-He Bu



Three H<sub>3</sub>BTC-supported 3D MOFs with triangular M<sub>3</sub> (M = Co, Ni) clusters and rod-shaped sinusoidal-like Mn-chains as building units have been successfully obtained under solvothermal conditions, and complexes **1–3** exhibit antiferromagnetic behaviours.